Contract No:

This document was prepared in conjunction with work accomplished under Contract No. DE-AC09-08SR22470 with the U.S. Department of Energy.

Disclaimer:

Mass Transfer Coefficients for a Non-Newtonian Fluid and Water With and Without Anti-foam Agents

Robert A. Leishear
Savannah River National Laboratory
Aiken, South Carolina, 29803
803-725-2832, Robert.Leishear@SRNL.DOE.gov

Hector N. Guerrero
Savannah River National Laboratory
Aiken, South Carolina, 29803
803-725-4127, Hector.Guerrero@SRS.gov

Michael L. Restivo
Savannah River National Laboratory
Aiken, South Carolina, 29803
803-725-3355, Michael.Restivo@SRNL.DOE.gov

David J.Sherwood
Hanford Waste Treatment & Immobilization Plant Project
2435 Stevents Center Place
Richland, WA 99354

ABSTRACT

Mass transfer rates were measured in a large scale system, which consisted of an 8.4 meter tall by 0.76 meter diameter column containing one of three fluids: water with an anti-foam agent, water without an anti-foam agent, and AZ101 simulant, which simulated a non-Newtonian nuclear waste. The testing contributed to the evaluation of large scale mass transfer of hydrogen in nuclear waste tanks. Due to its radioactivity, the waste was chemically simulated, and due to flammability concerns oxygen was used in lieu of hydrogen. Different liquids were used to better understand the mass transfer processes, where each of the fluids was saturated with oxygen, and the oxygen was then removed from solution as air bubbled up, or sparged, through the solution from the bottom of the column. Air sparging was supplied by a single tube which was co-axial to the column, the decrease in oxygen concentration was recorded, and oxygen measurements were then used to determine the mass transfer coefficients to describe the rate of oxygen transfer from solution. Superficial, average, sparging velocities of 2, 5, and 10 mm/second were applied to each of the liquids at three different column fill levels., and mass transfer coefficient test results are presented here for combinations of superficial velocities and fluid levels.

KEYWORDS

Mass transfer coefficient, non-Newtonian fluid, Newtonian fluid, anti-foam agent, dissolved oxygen.

SYMBOLS

AFA	anti-foam agent
C(t)	dissolved oxygen concentration
Ca	oxygen concentration at equilibrium
*C**	dissolved oxygen concentration at saturation
DO	dissolved oxygen
K_La	mass transfer coefficient, minute^{-1}
t	time, minute
V_{sup}	superficial velocity, millimeter/second
μ	consistency, Pascal · second

INTRODUCTION

Bubble column mass transfer tests were performed to investigate gas retention and release in various liquids. The liquids included process well water, process water mixed with anti-foam agent (*AFA*) which was cloudy white in color (Dow Corning, Q2-3183, antifoam agent), and AZ101 simulant which was a reddish brown liquid. The liquids were tested in an 8.4 meter tall by 0.76 meter diameter column, shown in Figs. 1 and 2. The column was filled to various levels and the simulants were injected with oxygen to saturation through the mixing loop shown in Fig. 3. Once saturated, air was introduced through a concentric, vertical sparger tube to strip the oxygen from solution. Air removed oxygen from solution as it bubbled up from the bottom of the column through each simulant to the surface. Some mass transfer data is available in the literature (Maraio, et. al. [1], Bello, et. al. [2]), but mass transfer test data for large systems and the AZ101 fluid was unavailable.

In addition to mass transfer coefficients, void fractions and bubble formations were also considered in this research but are documented in other papers (Guerreo, et. al. [3], Leishear and Restivo, [4, 8]). This paper presents only the experimental mass transfer research to provide some insight into the effects of anti-foam agents and Newtonian or non-Newtonian fluid type on mass transfer coefficients. To evaluate the mass transfer coefficients, measurements of the pressure at various column levels, laser

measurements of the surface level, and dissolved oxygen concentration (*DO*) were recorded for the liquids at different superficial velocities. To support mass transfer calculations, a required definition for the mass transfer coefficient follows.

Figure 1: Column Installation for Water and AZ101 Testing

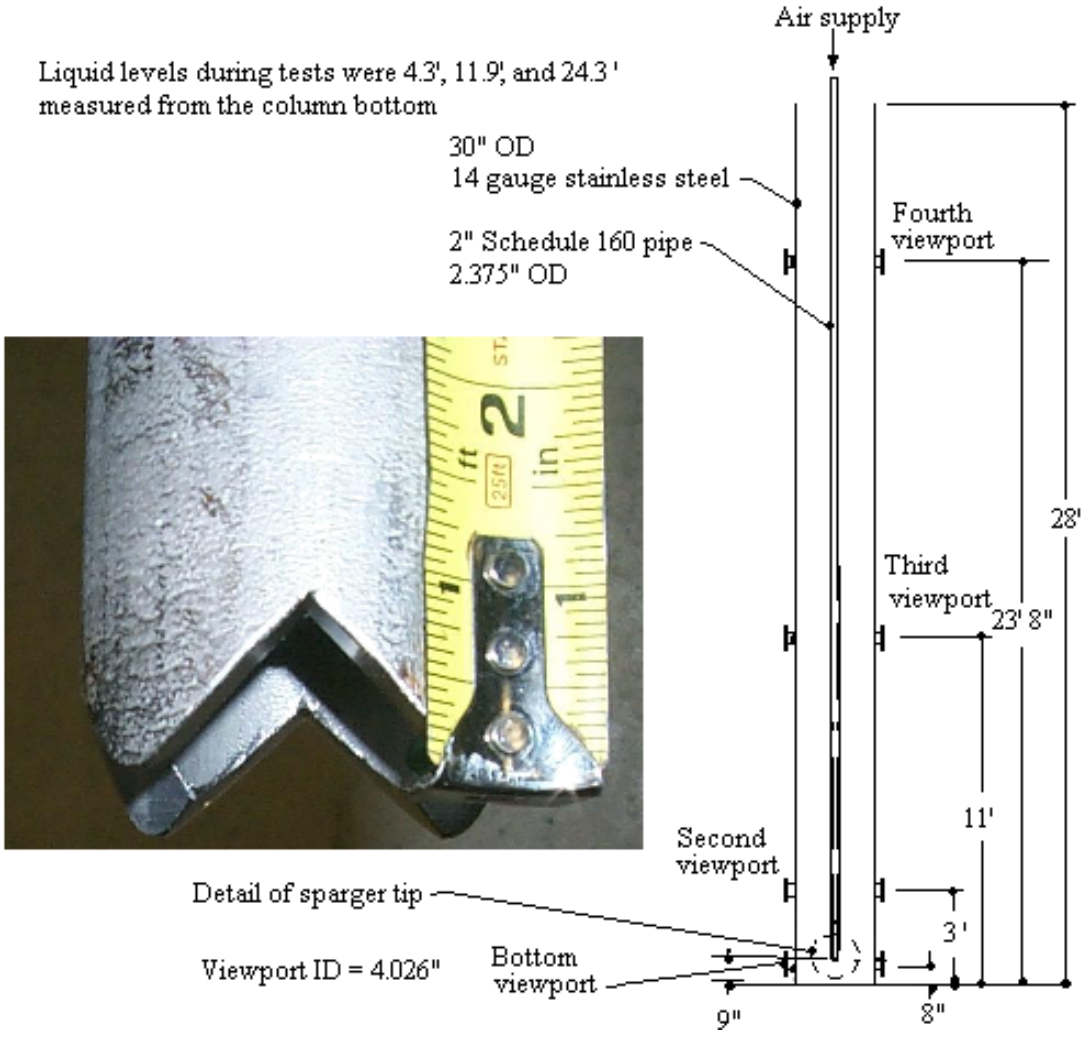

Figure 2: Column Details for Water and AZ101 Testing

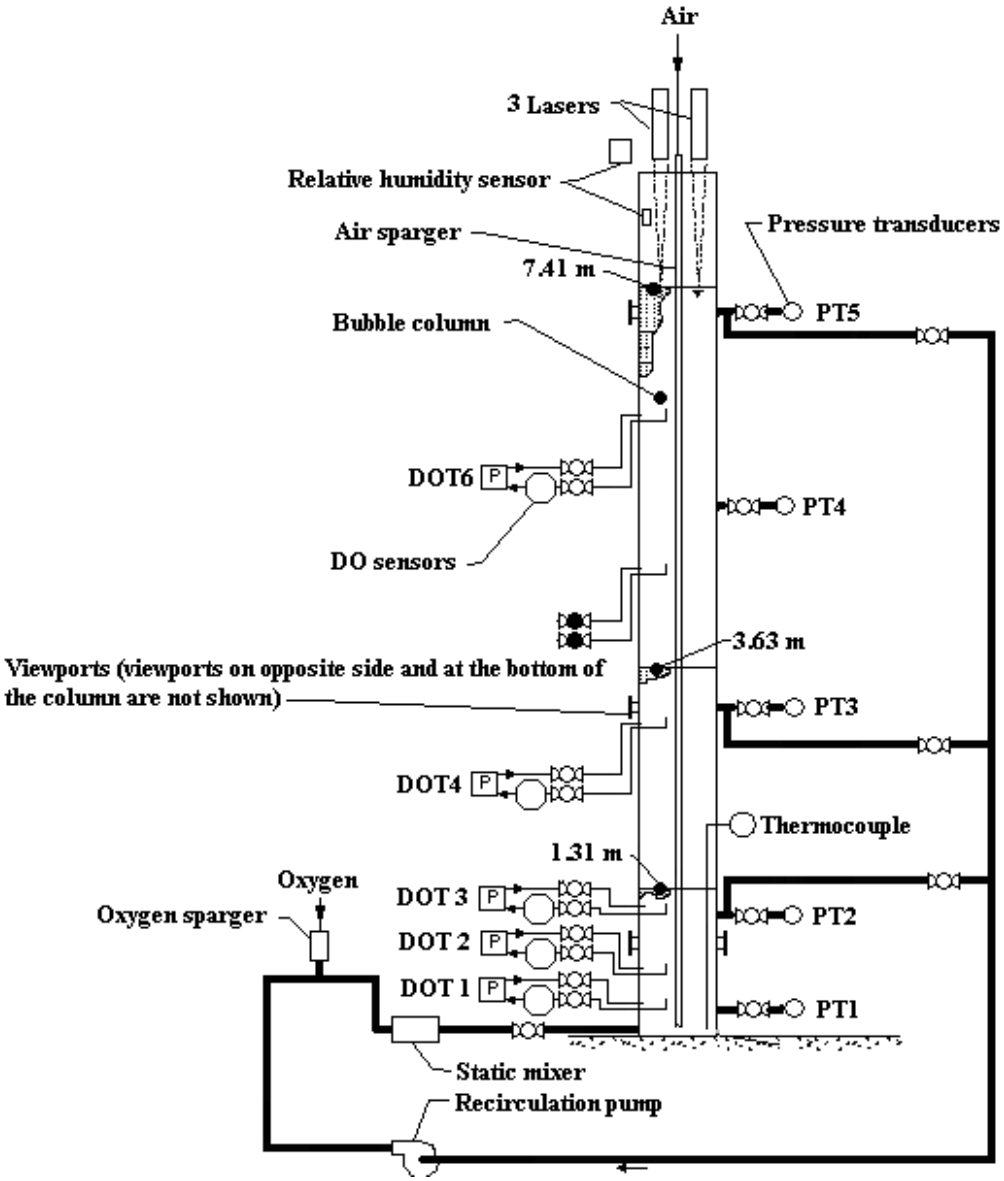

Figure 3: Equipment Schematic

MASS TRANSFER COEFFICIENT

The mass transfer equation is defined as (Yagi and Voshido [5])

$$\frac{dC(t)}{dt} = -k_L a \cdot (C(t) - Ca) \tag{1}$$

where

t – time

$C(t)$ – dissolved oxygen concentration,

Ca – oxygen concentration at equilibrium,

*C** - dissolved oxygen concentration at saturation,

$K_L a$ – mass transfer coefficient.

Integrating,

$$\frac{C(t)-Ca}{C^*-Ca} = \exp(-k_L a \cdot t) \tag{2}$$

and solving for the mass transfer coefficient

$$k_L a = -\frac{1}{t} \cdot ln\left(\frac{C(t)-Ca}{C^*-Ca}\right) \tag{3}$$

Mass transfer coefficients are experimentally evaluated using Eq. 3, where the terms *C** and *Ca* are experimentally determined constants. Once these constants are known, the change in concentration, *C*, is measured with respect to time, and $K_L a$ is plotted as a straight line with respect to time, such that $y = m \cdot t + b$, where y equals the natural log term in Eq. 3, $m = -K_L a$, and *b* is experimentally determined during test. The mass transfer coefficients are then determined from the slope of the straight line plots of experimental results. To explain how the plots are obtained, an equipment description is first provided.

EQUIPMENT DESCRIPTION AND FLUID PROPERTIES

The tests for the water and AZ101 tests can be described using Fig. 3. Oxygen is added to the liquid using the mixing loop, and once the liquid is saturated, the mixing loop is isolated from the column and air sparging is started. Then the change in *DO* concentration is measured.

Fluids

The AZ101 solution is a mixture of chemicals and metals used to simulate nuclear waste, which also includes anti-foam agent (Guerrero, et. al. [3]). Although some settling of solids occurs during mixing, the simulant exhibits macroscopic fluid properties. To obtain rheological fluid properties for the AZ101, a rheometer was used to display typical data as shown in Fig. 4, where two curves are obtained as the rheometer torque is increased (up) or decreased (down). For the water tests, process well water was used, which contains some minor quantities of minerals. *AFA* was added at 350 mg/liter for each fluid.

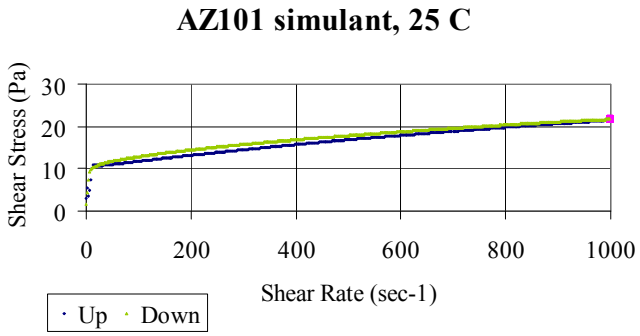

Figure 4: Fluid Properties

Oxygen Addition

The liquids are recirculated through one of the three column outlets shown on the right side of the column in Fig. 3. The fluid exits the column near the liquid surface and enters the recirculation pump. Then oxygen micro-bubbles are added to solution through a sintered metal filter (oxygen sparger) and are thoroughly mixed using a static mixer shown in Fig.5. Similar oxygen additions were performed for the other two opaque liquids. Once a liquid was saturated, valves to the column were closed, and air addition was started.

Figure 5: Installed Static Mixer

Air Sparging

Air was added through the sparge tube shown in Fig. 2, flow rates were adjusted to obtain the appropriate superficial velocities, and observed bubble formation was notably different, depending on whether the fluid was Newtonian or not. In water and water with AFA, a cone of bubbles formed at the sparger tip as shown in Fig. 6. As the bubbles rose in the column of water the bubbles became uniformly distributed as shown in Fig. 7, where most of the 1/4 to 3/8 inch diameter bubbles moved up through the center of the column, while some of the bubbles re-circulated down along the inner column surface. Bubble diameters were not discernible in the opaque water with AFA, but the surface bubbles were comparable to those observed in water. In AZ101, large bubbles were formed instead of many smaller bubbles as shown in Fig. 8. Depending on the air flow rate, the bubbles in AZ101 varied from 4 to 18 inches in diameter.

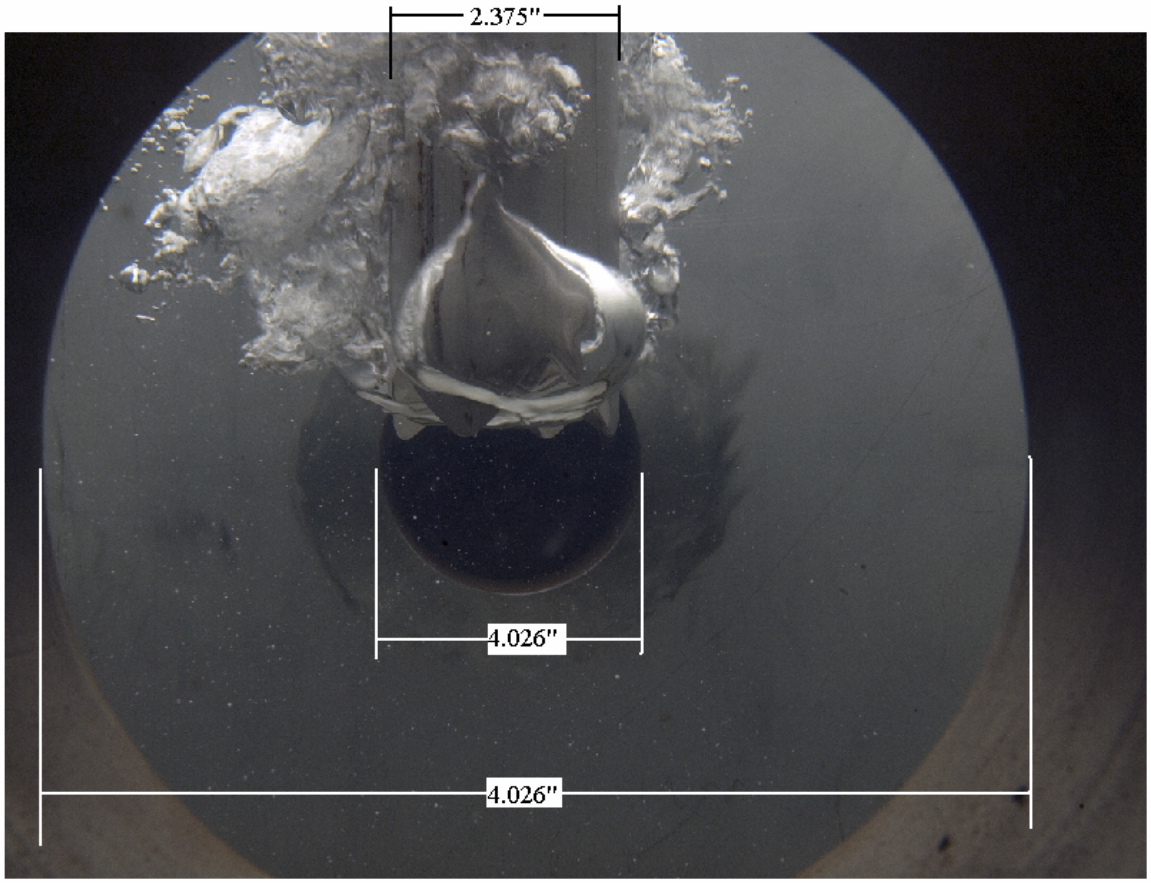

Figure 6: Formation of a Cone of Bubbles at the Sparger in Water, Viewed at the Bottom Viewport

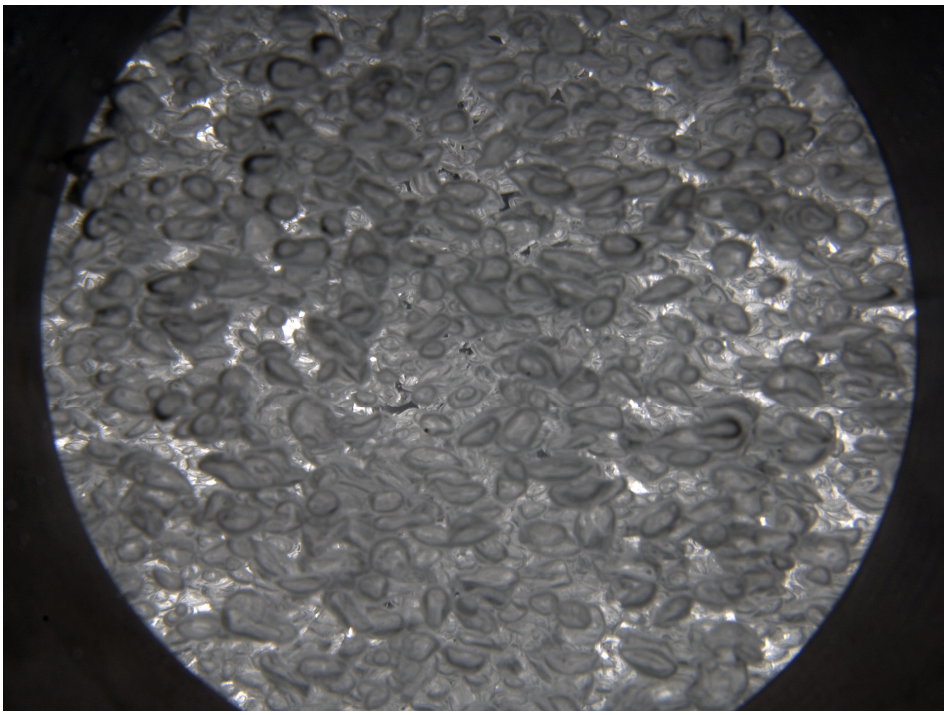

Figure 7: Uniform Distribution as the Bubbles Rise in Water, Viewed at a Higher Viewport

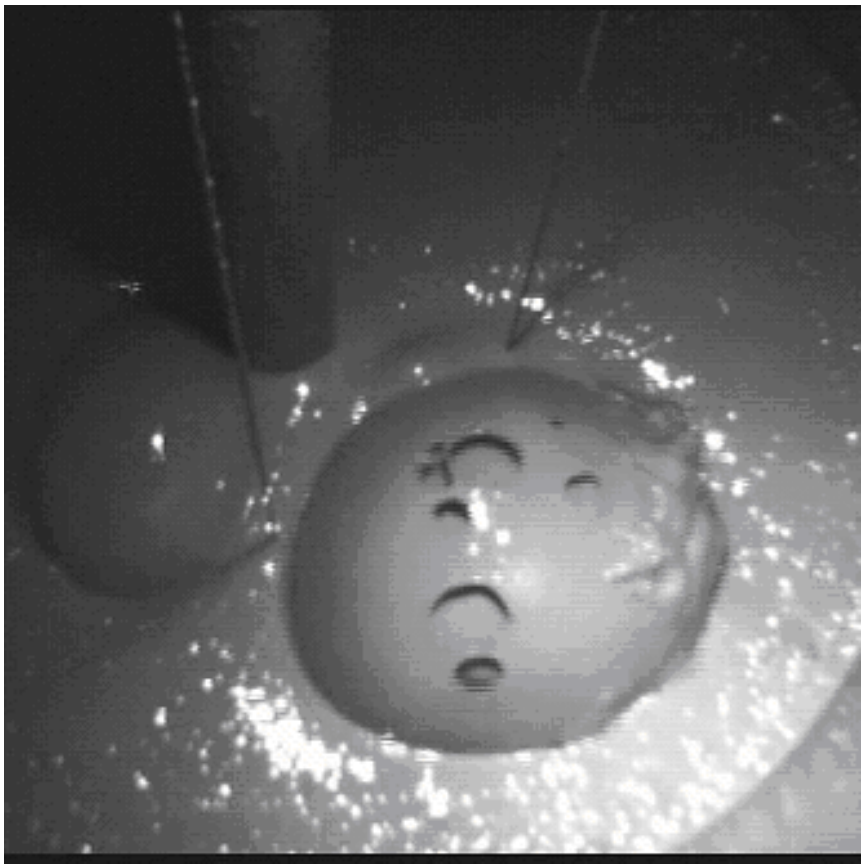

Figure 8: Bubble Formation in AZ101, Viewed from the Top of the Column

DO Equipment

DO measurements were obtained continuously during oxygen addition and subsequent air sparging. DO polarographic sensor operation is based on the electrical potential between two electrodes within the sensor. The electrodes are enclosed by a Tefzel membrane, and a zero oxygen solution (electrolyte) fills the void between a membrane and the electrodes. The solution will not maintain oxygen in solution, but oxygen can pass through the solution to the electrodes. The oxygen pressure at the surface of the membrane provides a motive diffusion force to drive oxygen into solution toward the chemical reaction, which occurs at the electrodes.

Henry's Law relates the partial pressure of oxygen at the fluid surface in the column to the parts per million, ppm, of oxygen dissolved in water at ambient conditions (23º – 28º C. When water is exposed to air, the concentration is related to the pressure and temperature, using Henry's Law, such that $C(t) = P/H$, where $C(t)$ is the concentration as a function of time, t, P is the partial pressure of the gas (oxygen), and H is Henry's constant. This relationship was used to establish calibration for the sensors, using pure oxygen at different pressures. DO sensor errors were noted to be approximately ± 2 ppm throughout the range of interest. Errors associated with rise time of the sensors were neglected.

RESULTS

Tests were performed at three different fluid levels (1.31 meters, 3.63 meters, and 7.41 meters) and three different superficial velocities at each fluid level. Superficial velocities of 2, 5, and 10 millimeter/second corresponded to sparger flow rates 2.1, 5.2, and 10.5 scfm, respectively. For each of the tests, DO measurements were used to obtain mass transfer coefficients.

DO Measurements.

DO measurements are shown in Figs. 9 and 10. Figure 9 displays results that are typical of all water tests, all water with AFA tests, and most of the AZ101 tests. However, near the bottom of the column, DO concentrations change as shown in Fig. 10. Note that the mass flow rate of oxygen from solution significantly decreased at the lower level, where oxygen is trapped in solution due to inadequate mixing. The mass transfer coefficients differed by as much as a factor of seven near the bottom of the column.

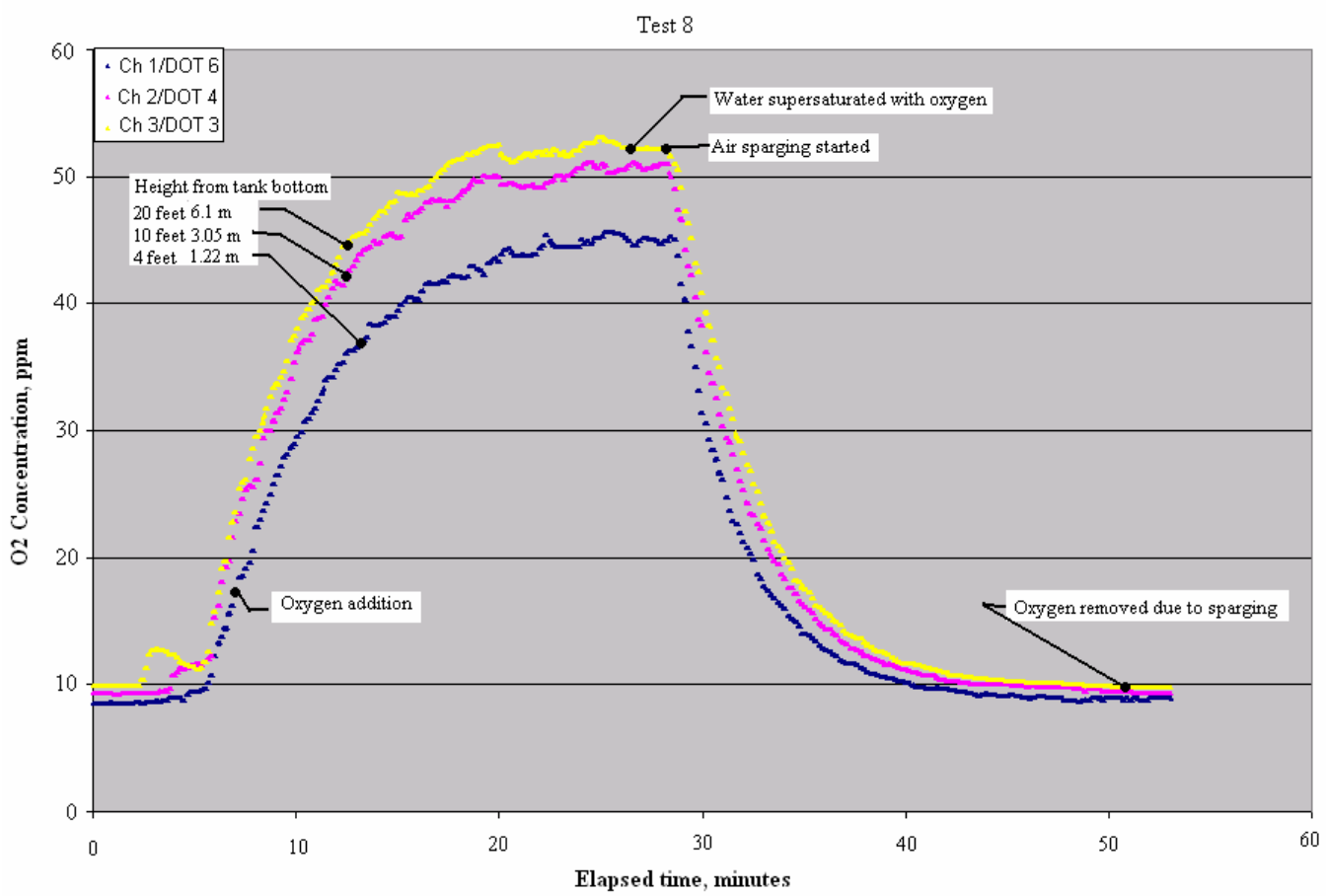

Figure 9: Typical DO Measurements

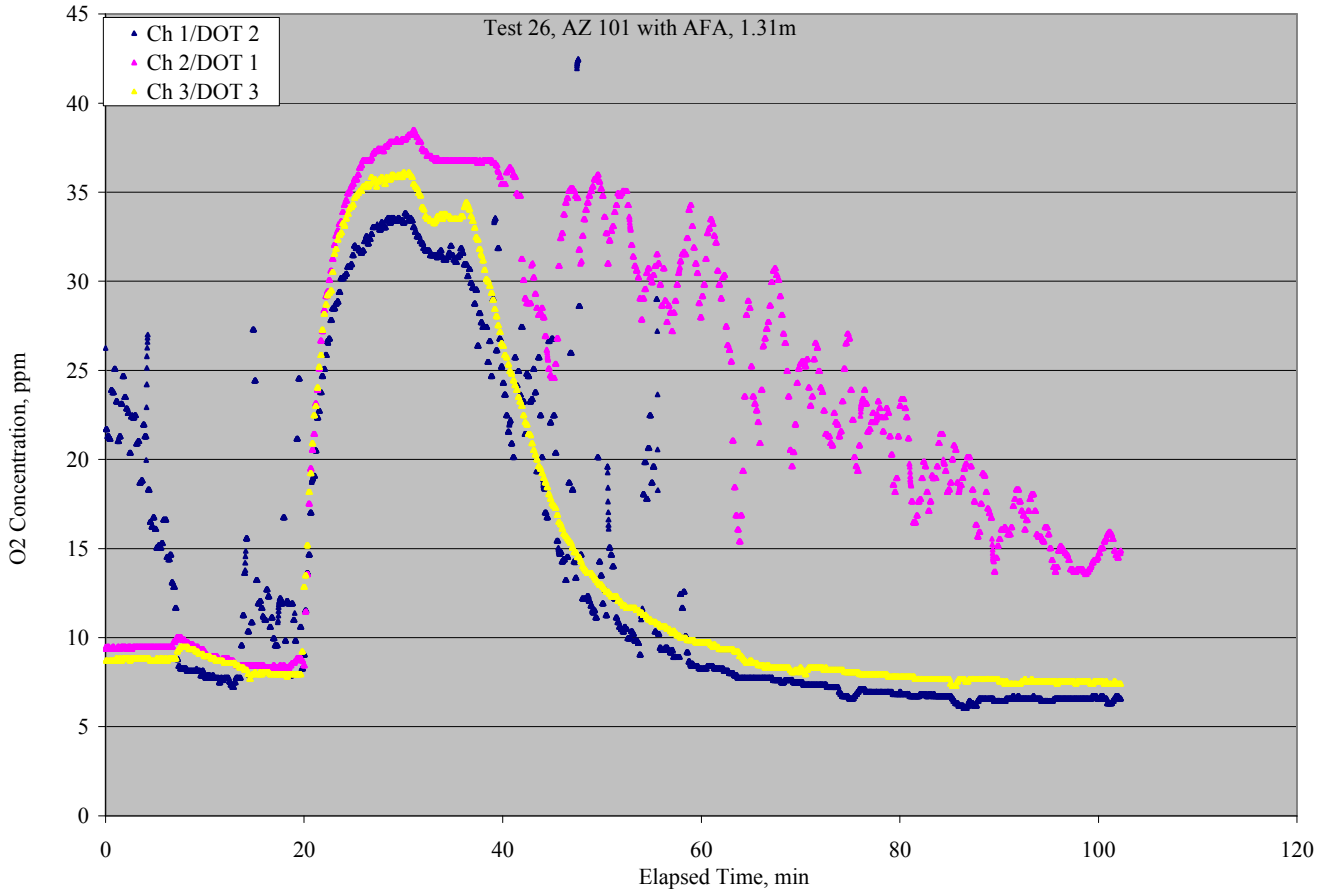

Figure 10: Atypical DO Measurements Near the Bottom of the Column

Mass Transfer Coefficient Calculations

Using Eq. 3 and DO sensor data, the mass transfer coefficients were calculated. Consistent with the observations for DO data, the mass transfer coefficients were linear for water, water with AFA, and AZ101 simulant, except near the bottom of the column for AZ101 testing. A representative result for most tests is shown in Fig. 11, and one of the results near the column bottom for AZ101 is shown in Fig. 12. Data at the bottom of the column was neglected in calculations for mass transfer coefficients, since results are markedly scattered and uncorrelated near the column bottom.

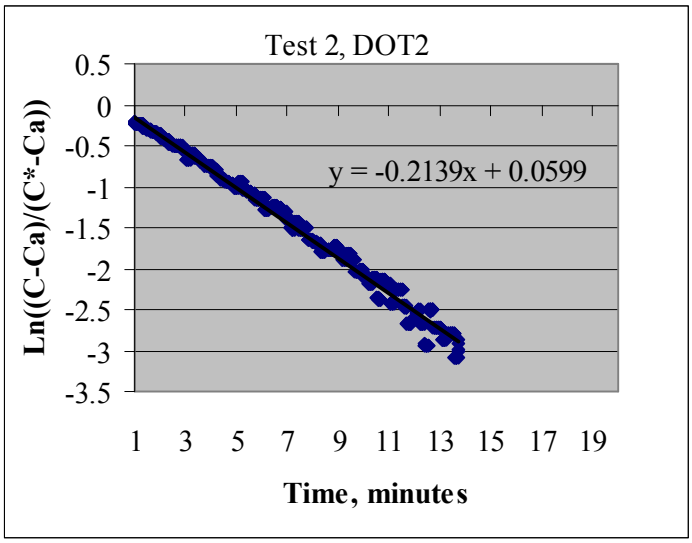

Figure 11: Typical Mass Transfer Calculation

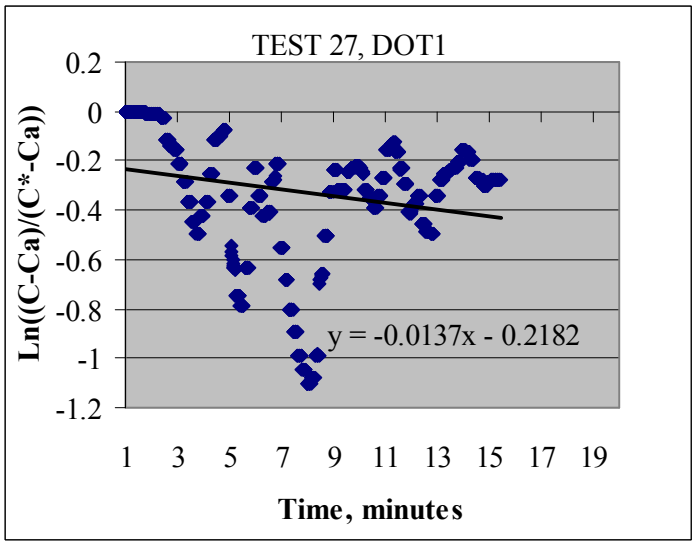

Figure 12: Atypical Mass Transfer Calculation, Near the Column Bottom

Mass Transfer Coefficients

Graphic displays of the mass transfer testing are provided in Figs. 13 – 19. In all cases, k_La is lower when the simulant contains AFA. The plot of k_La versus superficial velocity, Vsup, was expected to be linear. The nonlinearity is probably associated with the fact that the mass transfer equation assumes that the bubbles are distributed uniformly as they rise. In the lower meter of the column, the cone of bubbles from the sparger is created as waves of bubbles pass through the non-uniform flow field. In addition, secondary

flows exist outside of the cone of bubbles. Together, these conditions create a flow field dissimilar from the tacit assumptions of Eq. 3.

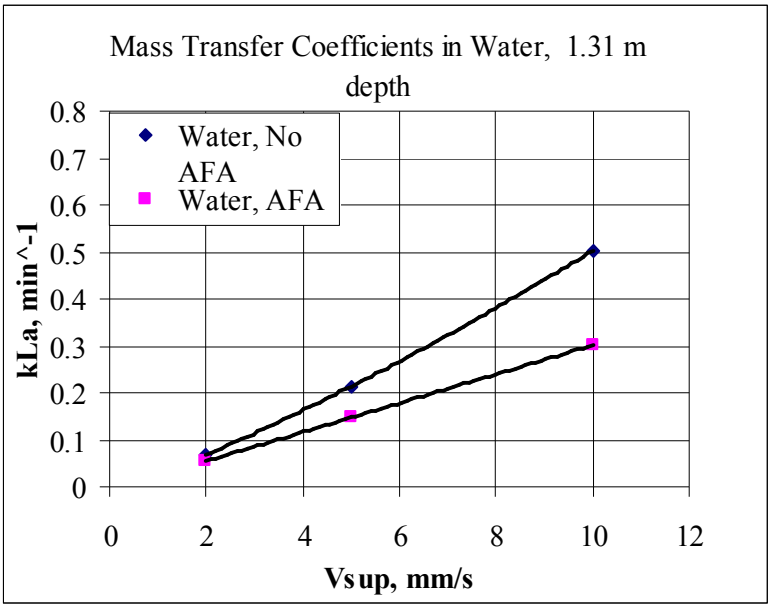

Figure 13: Mass Transfer Coefficients for Tests in Water for 1.31m Depth

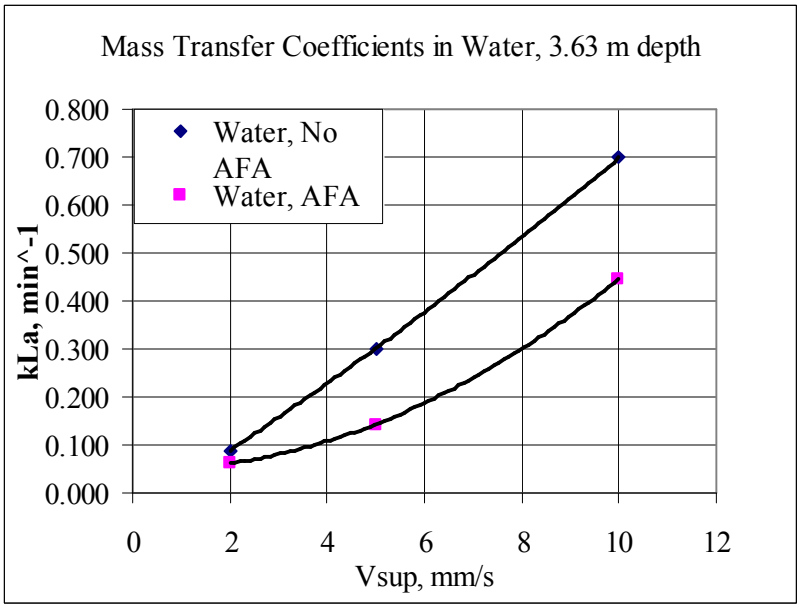

Figure 14: Mass Transfer Coefficients for Tests in Water in 3.63m Depth

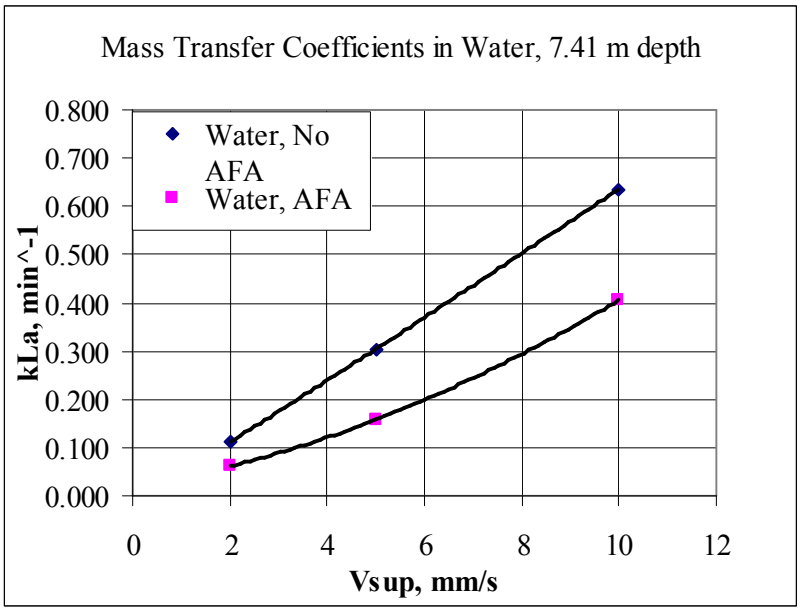

Figure 15: Mass Transfer Coefficients for Tests in Water for 7.41m Depth

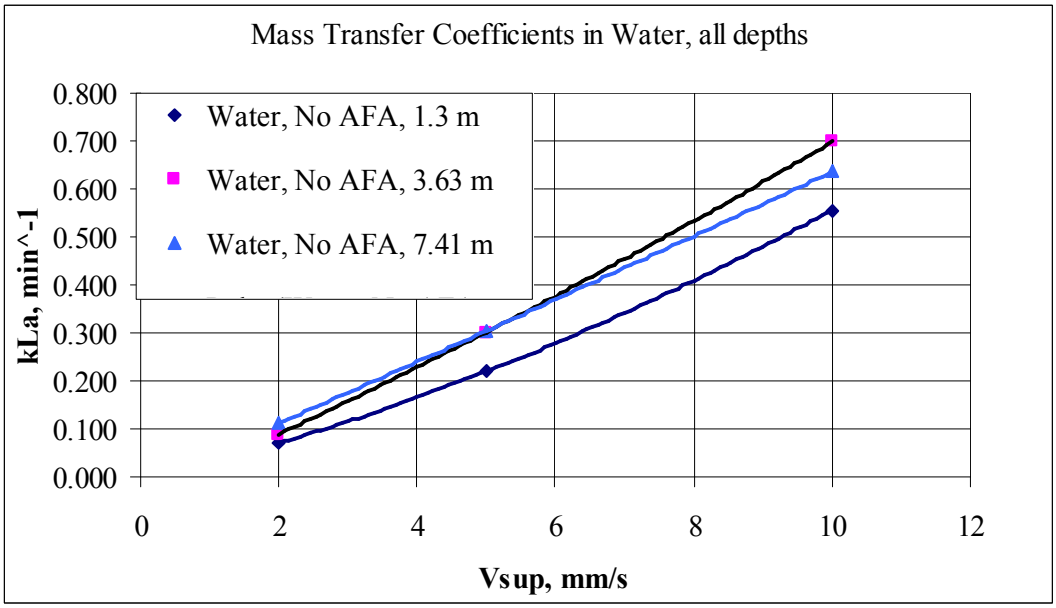

Figure 16: Mass Transfer Coefficients for Tests in Water, No AFA, for Different Depths

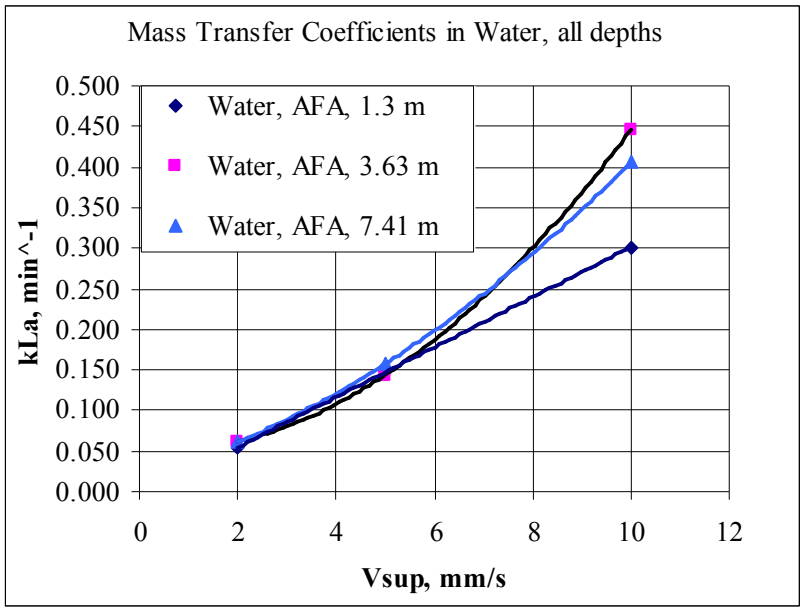

Figure 17: Mass Transfer Coefficients for Tests in Water with AFA for Different Column Depths

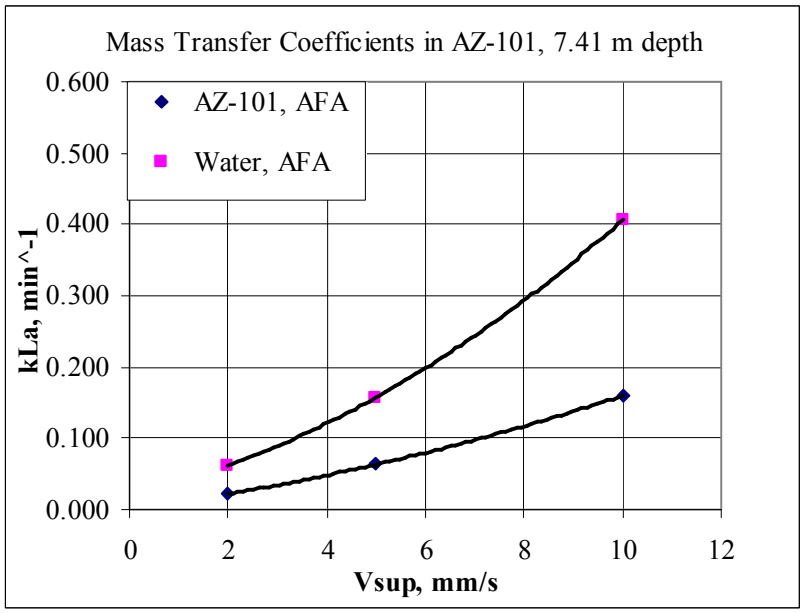

Figure 18: Comparison of Mass Transfer Coefficients in Water and AZ-101 Fluid with AFA for 7.41 m Depth

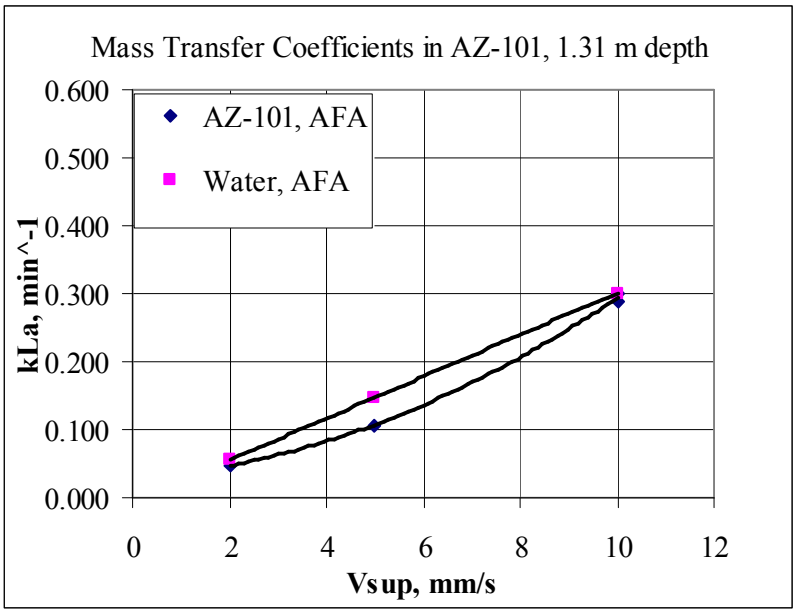

Figure 19: Comparison of Mass Transfer Coefficients in Water and AZ-101 Fluid with AFA for 1.31 m Depth

Comparison of Current Theory to Experimental Results for Mass Transfer Coefficients

Mass transfer coefficients were compared to available theory for both the AZ101 and water simulants. One theory from Shah, et.al., [6] was compared to water both with and without AFA, and even though it neglects the effects of AFA, it is stated as

$$k_L a = 0.467 \cdot V_{sup}^{0.82} \tag{4}$$

where V_{sup} is the superficial velocity in meter / second. Shah's results were based on smaller columns with multiple spargers.

The other theory from Godbole, et. al., [7] was applied to the AZ101 simulant

$$k_L a = 8.35 \times 10^{-4} \frac{V_{sup}^{0.44}}{\mu^{1.01}} \tag{5}$$

where μ is the effective viscosity, and for this type of fluid is assumed to be the constant average slope, or cconsistency, of the shear stress / shear strain curve above ≈ 25 second^{-1}. Again the effects of AFA were not considered using this theory.

Results of the comparisons are shown in Figs. 20 – 22. Note that at the lowest superficial velocity (2 mm/second) the coefficients are similar for both water and water with AFA, and their values are about 40% of the predicted values. As the superficial velocity increases to 10 mm/second the coefficient converges to within 15% of the predicted values for water. However, for water with AFA the coefficients are 47 - 70 % of the predicted values. For the AZ101 simulant the errors are even more significant. At the lower 1.31 meter test level the error varies from a factor of 6 to a factor of 1.9 at 2 and 10 mm/second respectively. At the 7.41 meter column level the coefficients vary by factors of 13 to 3.6. Data comparisons for AZ101 with and without AFA are unavailable, but the AFA effects are inadequate to explain the disparity between theory and experiment. The large bubble sizes in the AZ101 and the mixing characteristics near the sparger are considered to be the cause of the disparity for AZ101.

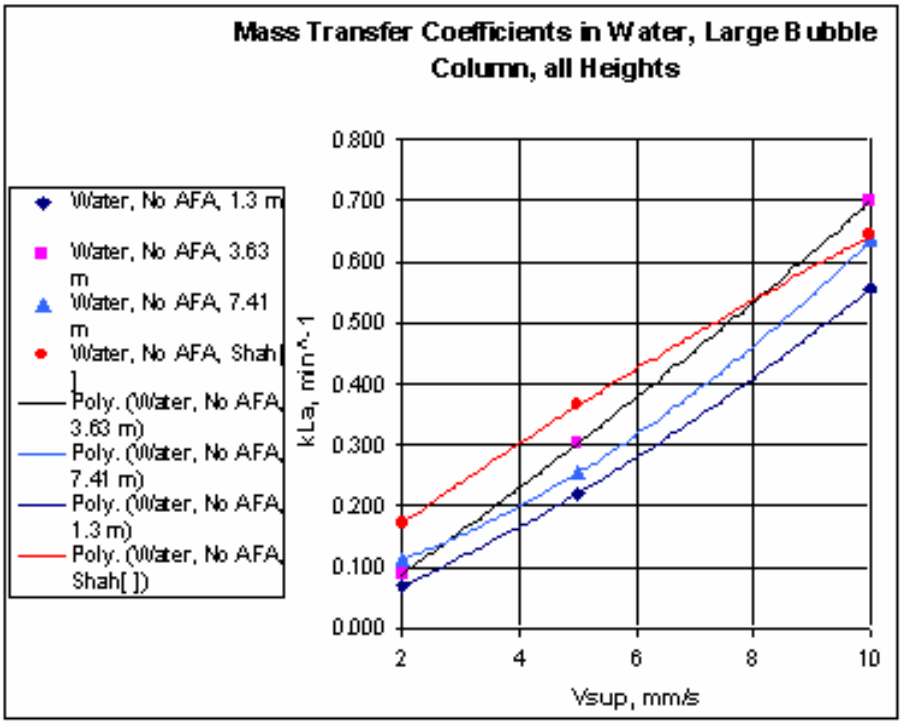

Figure 20: Comparison of Predicted Mass Transfer Coefficients to Experiments for Water without AFA

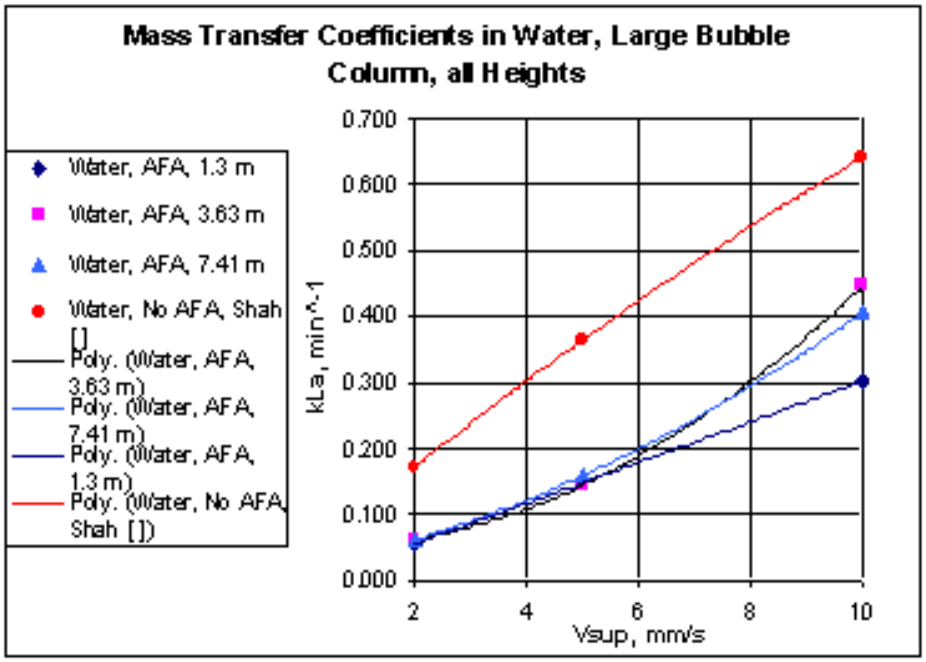

Figure 21: Comparison of Predicted Mass Transfer Coefficients to Experiments for Water with AFA

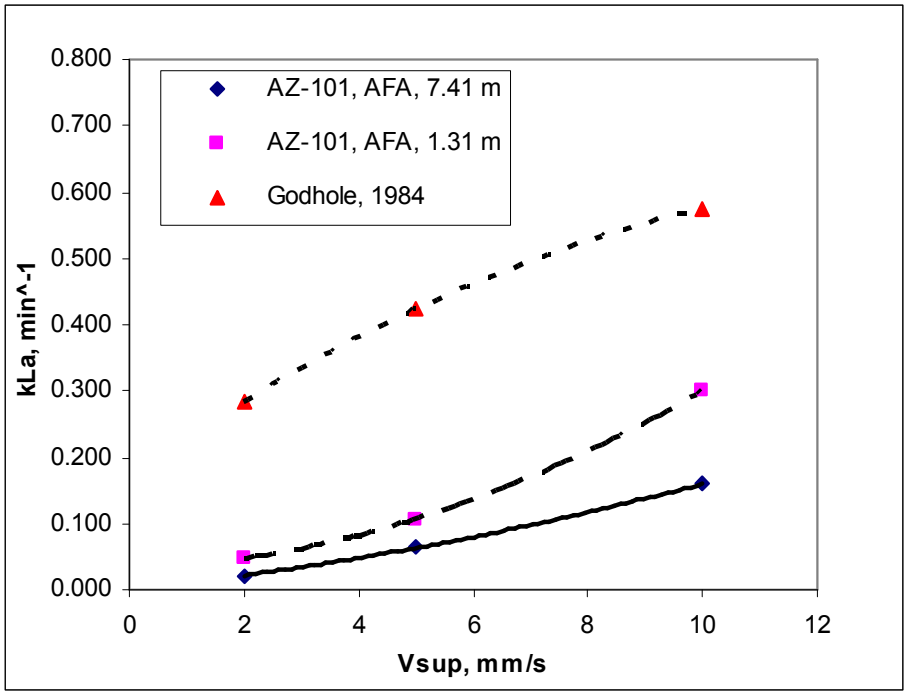

Figure 22: Comparison of Predicted Mass Transfer Coefficients to Experiments for AZ101 Fluid

CONCLUSION

Tests were performed in an 8.4 meter tall by 0.76 meter diameter column to investigate mass transfer coefficients and the effects of an antifoam agent in water and a manufactured radioactive liquid waste simulant, AZ101. Superficial velocities between 2 and 10 mm/second were applied at different levels in the column between 1.31 and 7.41 meters. The coefficients were consistently lower for water with AFA than for water without AFA, and the coefficients for the AZ101 were even lower.

The results were compared to current theory from the literature [9]. For water without AFA the mass transfer coefficients diverged from predictions by 15 to about 40 % of the predicted values as the superficial velocities decreased. For water with AFA the coefficients were typically 40 – 70 % of the predicted values. For AZ101 with AFA, the predicted coefficients were 3.6 to 13 times the experimental values. Accordingly, current models are inadequate for both low superficial velocities and Non-Newtonian fluids in large scale systems. In other words, scale up testing showed that existing models incorrectly predict results, and that experimental data is required to determine mass transfer coefficients for low superficial velocities or non-Newtonian fluids.

REFERENCES

[1] Morao, A., Maia, C. I., Fonseca, M. M. R., Vasconselos, J. M. T., Alves, S. S., "Effect of Antifoam Agent on Gas-Liquid Mass Transfer in Stirred Fermenters", Bioprocess Engineering, Springer-Verlag, pp. 165 – 172, 1999.

[2] Bello, R. A., Robinson, C. W., Moo-Young, M., "Prediction of the Volumetric Mass Transfer Coefficient in Pneumatic Contactors", Pergammon, Press, Great Britain, pp. 53 – 58, 1985.

[3] Guerrero, H. N., Crawford, C. L., Fowley, M. D., Leishear, R. A., Restivo, M. L., "Effects of Alternate Antifoam Agents, Noble Metals, Mixing Systems, and Mass Transfer on Gas Holdup and Release from Non-Newtonian Slurries", WSRC-TR-2007-00537, Savannah River National Laboratory, pp. 1 – 240, 2007.

[4] Leishear, R. A., Restivo, M., "Bubble Formation in a Large Scale System", FEDSM2008-55013, 2008 Fluids Conference, ASME, New York.

[5] Yagi, H. and Voshido, F., "Oxygen Absorption in Fermenters – Effects of Surfactants, Antifoaming Agents, and Sterilized Cells", Journal of Fermentation Technology, Vol. 53, no.12, pp. 905-916, 1974.

[6] Shah, Y. T, Kelkar, and Godbole, S. P., "Design Parameters Estimation for Bubble Column Reactors", AICHE Journal, Vol. 28, No. 3, May 1982, pp. 353-379.

[7] Godbole, S. P., Schumpe, A., and Shah, Y. T., "Hydrodynamics and Mass Transfer in Non-Newtonian Solutions in a Bubble Column", AICHE Journal, Vol. 30, No. 2, March, 1984, pp. 213-220.

[8] Leishear, R. A., Restivo, M., Guerrero, H. N., Sherwood, D. J., "Effects of Oxygen and Air Mixing on Void Fractions in a Large Scale System", 2008, AIChE Annual Conference.

[9] Shaikh, A. and Al-Dahhan, "A Review on Flow Regime Transition in Bubble Columns", International Journal of Chemical Reactor Engineering, Vol. 5, 2007.